

# Molecular tracing of SARS-CoV-2 in Italy in the first three months of the epidemic

Alessia Lai\*<sup>1</sup>, Annalisa Bergna<sup>1</sup>, Sara Caucci<sup>2</sup>, Nicola Clementi<sup>3</sup>, Iaria Vicenti<sup>4</sup>, Filippo Dragoni<sup>4</sup>, Anna Maria Cattelan<sup>5</sup>, Stefano Menzo<sup>2</sup>, Angelo Pan<sup>6</sup>, Annapaola Callegaro<sup>7</sup>, Adriano Tagliabracci<sup>8</sup>, Arnaldo Caruso<sup>9</sup>, Francesca Caccuri<sup>9</sup>, Silvia Ronchiadin<sup>10</sup>, Claudia Balotta<sup>1</sup>, Maurizio Zazzi<sup>4</sup>, Emanuela Vaccher<sup>11</sup>, Massimo Clementi<sup>3</sup>, Massimo Galli<sup>1</sup>, Gianguglielmo Zehender<sup>1</sup> on behalf of SARS-CoV-2 ITALIAN RESEARCH ENTERPRISE – (SCIRE) collaborative Group

<sup>1</sup> Department of Biomedical and Clinical Sciences Luigi Sacco, University of Milan, Milan, Italy.

<sup>2</sup> Department of Biomedical Sciences and Public Health, Virology Unit, Polytechnic University of Marche, Ancona, Italy.

<sup>3</sup> Microbiology and Virology Unit, "Vita-Salute" San Raffaele University, Milan, Italy.

<sup>4</sup> Department of Medical Biotechnologies, University of Siena, Siena, Italy.

<sup>5</sup> Infectious Diseases Unit, Department of Internal Medicine, Azienda Ospedaliera-Universitaria di Padova, Padua, Italy.

<sup>6</sup> Infectious Diseases, ASST Cremona, Cremona (MI), Italy.

<sup>7</sup> Microbiology and Virology Laboratory, ASST Papa Giovanni XXIII, Bergamo, Italy.

<sup>8</sup> Section of Legal Medicine, Università Politecnica delle Marche, Ancona, Italy.

<sup>9</sup> Microbiology Unit, Department of Molecular and Translational Medicine, University of Brescia and ASST Spedali Civili Hospital, Brescia, Italy.

<sup>10</sup> Intesa Sanpaolo Innovation Center – AI LAB, Turin, Italy

<sup>11</sup> Medical Oncology and Immune-related Tumors, Centro di Riferimento Oncologico di Aviano (CRO), IRCCS, Aviano 33081, Italy.

\*Correspondence: [alessia.lai@unimi.it](mailto:alessia.lai@unimi.it); Tel.: (+39) 0250319775

**Abstract:** The aim of this study is the characterization and genomic tracing by phylogenetic analyses of 59 new SARS-CoV-2 Italian isolates obtained from patients attending clinical centres in North and Central Italy until the end of April 2020.

All but one of the newly characterized genomes belonged to the lineage B.1, the most frequently identified in European countries, including Italy. Only a single sequence was found to belong to lineage B.

A mean of 6 nucleotide substitutions per viral genome was observed, without significant differences between synonymous and non-synonymous mutations, indicating genetic drift as a major source for virus evolution.

tMRCA estimation confirmed the probable origin of the epidemic between the end of January and the beginning of February with a rapid increase in the number of infections between the end of February and mid-March. Since early February, an effective reproduction number ( $R_e$ ) greater than 1 was estimated, which then increased reaching the peak of 2.3 in early March, confirming the circulation of the virus before the first COVID-19 cases were documented.

Continuous use of state-of-the-art methods for molecular surveillance is warranted to trace virus circulation and evolution and inform effective prevention and containment of future SARS-CoV-2 outbreaks.

**Keywords:** Phylodynamic analyses; SARS-CoV2 circulation in Italy; molecular tracing; Whole Genome Sequencing.

49 **1. Introduction**

50 Italy is one of the countries most and earlier affected in Europe by the COVID-19 pandemic  
51 ([https://gisanddata.maps.arcgis.com/apps/opsdashboard/index.html#/bda7594740fd40299423467b48](https://gisanddata.maps.arcgis.com/apps/opsdashboard/index.html#/bda7594740fd40299423467b48e9ecf6)  
52 [e9ecf6](https://gisanddata.maps.arcgis.com/apps/opsdashboard/index.html#/bda7594740fd40299423467b48e9ecf6)). The first autochthonous cases of Coronavirus 2019 Disease (COVID-19) were observed  
53 starting from February 21, 2020 in Codogno (Lodi province), determining on February 22, 2020 the  
54 establishment of a 'red zone' to contain the epidemic, encompassing 11 municipalities. Thereafter, in  
55 a short time, it became evident that the epidemic had already involved a large part of Lombardy  
56 region and then spread to neighbouring regions and, substantially less, to the rest of the country. On  
57 March 9, lockdown was declared for the entire country. The rapidly increasing number of patients  
58 who required hospitalization in the intensive care unit suggested that the virus may have circulated  
59 for a long period and caused thousands of contagions before the epidemic became manifest [1].

60 SARS-CoV-2 was first detected in Italy in a couple of Chinese tourists coming from Wuhan on  
61 January 31 [2]. Subsequent evaluations have not shown a relationship between the sequence of these  
62 strains and those implicated in the epidemic in Lombardy [3].

63 On the contrary, the Codogno strains resulted strictly related with a strain of SARS-CoV-2  
64 coming from Shanghai which caused a small outbreak in Munich around January 20 [1] and was  
65 probably spread later to other European countries and beyond the Atlantic [4]. These sequences are  
66 part of a clade initially defined as a European clade, the old Nexstrain A2a subclade, which is  
67 currently the most widespread outside China and probably responsible for most of the world  
68 pandemic [5].

69 In the face of more than 240,000 notified cases in Italy, the entire genomes available in public  
70 databases are still scarce (77 at the time of this study). The availability of large numbers of sequences  
71 collected over time is necessary for molecular surveillance of the epidemic and for evaluation and  
72 planning of effective control strategies. To perform this study, a network of Italian Clinical centres  
73 and Laboratories across Italy generated additional 59 full-length SARS-CoV-2 sequences from  
74 COVID-19 patients ranging from the end of February to the end of April. This contribution helps to  
75 trace the temporal origin, the rate of viral evolution and the population dynamics of SARS-CoV-2 in  
76 Italy by phylogeny.

77 **2. Materials and Methods**

78 *2.1 Patients and Methods*

79 A total of 59 SARS-CoV-2 whole genomes were newly characterized from an equal number of  
80 patients affected by COVID-19, attending different clinical centres in Northern and Central Italy, from  
81 the beginning of the epidemic (February 22, 2020) until April 27, 2020 (Table S1).

82 All of the data used in this study were previously anonymised as required by the Italian Data  
83 Protection Code (Legislative Decree 196/2003) and the general authorisations issued by the Data  
84 Protection Authority. Ethics Committee approval was deemed unnecessary because, under Italian law,  
85 all sensitive data were deleted and we collected only age, gender and sampling date (Art. 6 and Art. 9  
86 of Legislative Decree 211/2003).

87 Eighteen sequences were obtained after isolating the virus in Vero E6 cells while the remaining 41  
88 were obtained directly from biological samples such as nasopharyngeal swabs or broncho-alveolar  
89 lavages (39 and 2, respectively).

90 SARS-CoV-2 RNA was extracted using the Kit QIAasymphony DSP Virus/Pathogen Midi kit on  
91 the QIAasymphony automated platform (QIAGEN, Hilden, Germany) (n=9) and manually with  
92 QIAamp Viral RNA Mini Kit (n=50).

93 Full genome sequences were obtained with different protocols by amplifying 26 fragments as  
94 previously described (n=42) [1] or using random hexamer primers (n=8) or Ion AmpliSeq SARS-CoV-2  
95 Research Panel (Thermo Fisher Scientific) (n=9). The PCR products were used to prepare a library for  
96 Illumina deep sequencing using a Nextera XT DNA Sample Preparation and Index kit (Illumina, San  
97 Diego, California, USA) in accordance with the manufacturer's manual, and sequencing was carried  
98 out on a Illumina MiSeq platform for fifty samples, while the remaining nine were sequenced on Ion

99 GeneStudio™ S5 System (Thermo Fisher Scientific) instrument following the Ion AmpliSeq™ RNA  
100 libraries protocol. The results were mapped and aligned to the reference genome obtained from  
101 GISAID (<https://www.gisaid.org/>, accession ID: EPI\_ISL\_412973) using Geneious software, v. 9.1.5  
102 (<http://www.geneious.com>) [6] or Torrent Suite v. 5.10.1 or BWA-mem and rescued using Samtools  
103 alignment/Map (v 1.9).

104

## 105 *2.2 Sequence data sets*

106 The newly characterized 59 genomes plus three previously characterized isolates by us  
107 (EPI\_ISL\_417445-417447) [1] were aligned with a total of 77 Italian sequences available in public  
108 databases (GISAID, <https://www.gisaid.org/>) on May 13, 2020 and 452 genomes sampled in different  
109 European and Asian countries (513 and 16, respectively) representing all the different viral clades  
110 described in the Nextstrain platform (<https://nextstrain.org/>). The final data set thus included 588  
111 sequences. Due to the large amount of available sequences, we focused the analysis on European  
112 strains by randomly selecting sequences from each country and by excluding identical strains or  
113 strains with more than 5% of gaps. We sampled the data in order to have no temporal gaps, by  
114 grouping the sequences by country/week/clade and randomly selecting the sequences in each group.  
115 We choose 15 sequences for clade A2 and 5 sequences for other clades for each European country. For  
116 countries with less than the required sequence number we kept all the sequences. The sampling dates  
117 of the entire dataset ranged from December 30, 2019 to April 27, 2020. Table S2 shows the accession  
118 IDs, sampling dates and locations of the sequences included in the dataset.

119 A subset of sequences assigned to the old Nextstrain A2 clade was generated for dating the  
120 epidemic, including all the Italian sequences, one German (EPI\_ISL\_406862) and three Chinese isolates  
121 from Shanghai, ancestral to the A2 clade (EPI\_ISL\_416327, EPI\_ISL\_416334 and EPI\_ISL\_416386).  
122 Coalescent and birth-death phylodynamic analyses were performed on the 136 Italian A2 sequences  
123 only.

124 Alignment was performed using MAFFT [7] and manually cropped to a final length of 29,779 bp  
125 using BioEdit v. 7.2.6.1 (<http://www.mbio.ncsu.edu/bioedit/bioedit.html>).

126

## 127 *2.3 Genetic distance, recombination and selection pressure analyses*

128 The MEGA X program was used to evaluate the genetic distance between and within Italian  
129 sequences on the full length genome, with variance estimation performed using 1,000 bootstrap  
130 replicates [8].

131 The RDP5 software was used to investigate the presence of potential recombination [9].

132 All of the genes were tested for selection pressure using Datamonkey  
133 (<https://www.datamonkey.org/>).

134

## 135 *2.4 Phylogenetic and phylodynamic analyses*

136 The simplest evolutionary model best fitting the sequence data was selected using the JmodelTest  
137 v.2.1.7 software [10], and proved to be the Hasegawa-Kishino-Yano model with a proportion of  
138 invariant sites (HKY+I).

139 The phylogenetic analysis for clade assignment was performed by RaxML [11] on the entire  
140 dataset of 588 genomes. During the period in which we were carrying out the study, the SARS-CoV-2  
141 clade nomenclature system changed. In particular, Rambaut et al. proposed a dynamic nomenclature  
142 based on phylogenetic lineages, called Pangolin (Phylogenetic Assignment of Named Global Outbreak  
143 LINeages) [12]. For this reason we used the old Nextstrain and the new Pangolin (freely available at  
144 <https://pangolin.cog-uk.io/>) systems for strain classification. The new Nextstrain classification was  
145 performed by using the available script  
146 (<https://github.com/nextstrain/ncov/blob/master/docs/running.md>).

147 The virus' phylogeny, evolutionary rates, times of the most recent common ancestor (tMRCA)  
148 and demographic growth were co-estimated in a Bayesian framework using a Markov Chain Monte  
149 Carlo (MCMC) method implemented in v.1.10.4 and v.2.62 of the BEAST package [13], [14].

150 A root-to-tip regression analysis was made using TempEst in order to investigate the temporal  
151 signal of the dataset [15].

152 Different coalescent priors (constant population size and exponential growth and Bayesian  
153 skyline) and strict *vs.* relaxed molecular clock models were tested by means of Path Sampling (PS) and  
154 Stepping Stone (SS) sampling [16]. The evolutionary rate prior normal distribution, after informing the  
155 mean evolutionary rate, was set at mean  $0.8 \times 10^{-3}$  substitutions/site/year  
156 (<http://virological.org/t/phylogenetic-analysis-176-genomes-6-mar-2020/356>).

157 The MCMC analysis was run until convergence with sampling every 10,000 generations.  
158 Convergence was assessed by estimating the effective sampling size (ESS) after 10% burn-in using  
159 Tracer v.1.7 software (<http://tree.bio.ed.ac.uk/software/tracer/>), and accepting ESS values of 200 or  
160 more. The uncertainty of the estimates was indicated by 95% highest marginal likelihoods estimated  
161 [17] by path sampling/stepping stone methods [16].

162 The final trees were summarised by selecting the tree with the maximum product of posterior  
163 probabilities (pp) (maximum clade credibility or MCC) after a 10% burn-in using Tree Annotator  
164 v.1.10.4 (included in the BEAST package), and were visualised using FigTree v.1.4.2  
165 (<http://tree.bio.ed.ac.uk/software/figtree/>).

166

### 167 *2.5 Birth-Death Skyline estimates of the effective reproductive number ( $R_e$ )*

168 The birth-death skyline model implemented in Beast 2.62 was used to infer changes in the  
169 effective reproductive number ( $R_e$ ), and other epidemiological parameters such as the death/recovery  
170 rate ( $\delta$ ), the transmission rate ( $\lambda$ ), the origin of the epidemic, and the sampling proportion ( $\rho$ ) [18].  
171 Given that the samples were collected during a short period of time, a “birth-death contemporary”  
172 model was used.

173 The analyses were based on the previously selected HKY substitution model and the  
174 evolutionary rate was set to the value of  $0.8 \times 10^{-3}$  subs/site/year, which corresponds to the mean  
175 substitution rate estimated using a relaxed clock under the exponential coalescent model as  
176 transformed into units per year.

177 For the birth-death skyline analysis, from one to two  $R_e$  intervals and a log-normal prior with a  
178 mean (M) of 0.0 and a variance (S) of 1.0 were chosen, which allows the  $R_e$  values to change between <1  
179 (0.193) to >5. A normal prior with M=48.7 and S=15 (corresponding to a 95% interval from 24.0 to 73.4)  
180 was used for the rate of becoming uninfected. These values are expressed as units per year and  
181 reflect the inverse of the time of infectiousness (5.3-19 days, mean 7.5) according to the serial interval  
182 estimated by Li *et al.* [19]. Sampling probability ( $\rho$ ) was estimated assuming a prior Beta (alpha=1.0 and  
183 beta=999), corresponding to a minority of the sampled cases (between  $10^{-5}$  to  $10^{-3}$ ). The origin of the  
184 epidemic was estimated using a normal prior with M=0.1 and S=0.05 in units per year.

185 The MCMC analyses were run for 100 million generations and sampled every 10,000 steps.

186 Convergence was assessed on the basis of ESS values (ESS >200). Uncertainty in the estimates was  
187 indicated by 95% highest posterior density (95%HPD) intervals.

188 The mean growth rate was calculated on the basis of the birth and recovery rates ( $r=\lambda-\delta$ ), and the  
189 doubling time was estimated by the equation: doubling time= $\ln(2)/r$  [20].

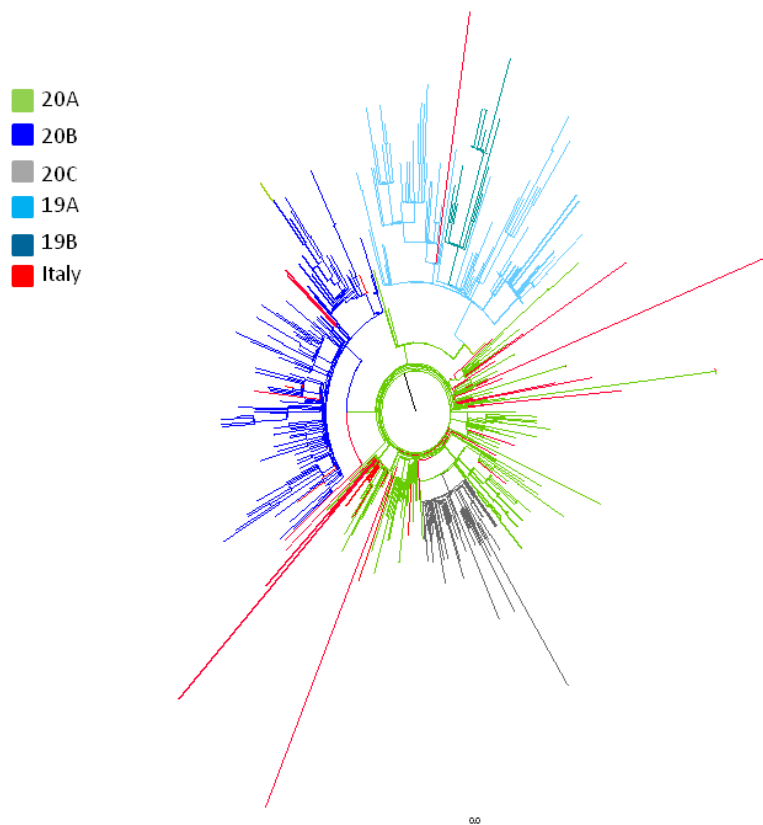
## 190 3. Results

### 191 *3.1 Phylogenetic analysis of the whole dataset*

192 No recombination events were observed in the entire dataset according to analyses with RDP5  
193 software.

194 Phylogenetic analysis by maximum likelihood showed that the Italian sequences were included  
195 in a single SARS-CoV-2 clade (the old Nextstrain A2 clade) with the exception of three sequences:  
196 two from Chinese patients visiting Italy at the end of January 2020 after being infected in Wuhan and  
197 one characterized by us from an Italian subject, living in Padua, sampled in March 2020, not  
198 reporting any recent trip outside Italy or contacts with subjects affected by COVID-19 (pp=0.99)  
199 (Figure 1, clade 19A).

200



201  
 202 Figure 1. Maximum likelihood tree of the full dataset including 588 SARS-CoV-2 genomes. Nextstrain  
 203 classification is indicated by colours as reported in the legend. Italian strains are highlighted in red.

204  
 205 Recently, new nomenclature systems have been proposed for the SARS-CoV-2 clades. The new  
 206 lineage assignment of 62 Italian isolates is reported on Table 1 with the correspondence to other  
 207 naming systems (old and new Nextstrain). All of our isolates belonged to the lineage B.1, only one  
 208 isolate was classified as lineage B.

209

210 Table 1. Pangolin lineage classification of 62 Italian strains included in the study.

211

Lineage (Pangolin)	Total	%	From	Nextstrain new	Nextstrain old
B	1	1.6	PD (1)	19A	nd
B.1	47	75.8	MI (15), PS(7), AN (1), MC (1) PD (8), BG (1), CR (3), SI (3), AR (3), GR (1), BS (4)	20A, nd	A2a
B.1.1	11	17.7	MI (4), PD (1), SI (4), GR (1), AR (1)	20B	A2a
B.1.34	1	1.6	MI (1)	nd	A2a
B.1.5	2	3.2	MI (1), BG (1)	20A	A2a

212 PD: Padua, MI: Milan, PS: Pesaro, AN: Ancona, MC: Macerata, BG: Bergamo, CR: Cremona, SI: Siena, AR: Arezzo, GR: Grosseto, BS: Brescia, nd: not determined.

213

214 3.2 Genetic distances analysis

215 The overall mean p-distance between all the Italian isolates was 2.3 (SE:0.3) s/10,000 nts,  
 216 corresponding to a mean of 6.4 (SE: 0.8) substitutions per genome. The non-synonymous distance  
 217 (dN) was 2.0 (SE: 0.4) non-syn s/10,000 non-syn nts while the overall synonymous mean distance  
 218 (dS) was equal to 2.4 (SE: .05) syn s/10000 syn nts (dN/dS=0.83). A higher heterogeneity was  
 219 observed through months as, stratifying the genetic distances on the basis of the sampling time, we  
 220 observed a higher heterogeneity among the strains isolated in February (n=19) compared to those  
 221 collected in March (n=96) or April (n=21) (Table 2).

222

223 Table 2. Mean genetic divergence within and between Italian strains according to the sampling time  
 224 (substitutions per 10,000 sites).

225

Time	Within				Time	Between			
	P distance (SE)	nucleotide (SE)	dS (SE)	dN (SE)		P distance (SE)	nucleotide (SE)	dS (SE)	dN (SE)
February	3.8 (0.6)	9.6 (1.5)	3.5 (1.1)	3.8 (0.6)	February vs March	3.1 (0.4)	8.1 (1.3)	2.9 (0.8)	2.8 (0.4)
March	1.9 (0.3)	5.4 (0.8)	2.2 (0.5)	1.5 (0.4)	March vs April	2.3 (0.3)	6.6 (0.8)	2.1 (0.6)	2.0 (0.5)
April	2.4 (0.3)	6.8 (0.9)	1.7 (0.8)	2.1 (0.5)	February vs April	3.7 (0.5)	10 (1.5)	2.7 (0.8)	3.5 (0.6)

226 SE: Standard error, dS: synonymous distance, dN: non-synonymous distance.

227

228 3.3 Differences in Amino Acids

229 Considering only the non-synonymous mutations and comparing the Italian genomes with the  
 230 common ancestor (China), there were 159 amino acid substitutions affecting different viral genes,  
 231 (112 in ORF 1a/1b, 19 in S, 12 in ORF 3a, 4 in M, 3 in ORF7a, 6 in N, and one each in Orf7b, 8 and 10)  
 232 of which only 15 (9.4%) were observed in 2 or more isolates, as summarized in Table 3. No  
 233 aminoacid changes were observed in the E gene. The previously described substitution D614G in the  
 234 Spike protein was present in all the isolates belonging to the lineage B.1 and in the strain from Padua  
 235 belonging to lineage B.

236 Considering the Italian isolates, only 1 site resulted under significant selecting pressure by three  
 237 different methods (MEME, FEL, FUBAR): site 1,046 in the S gene that was present in three isolates  
 238 from Padua. This G1046V mutation is located in the S2 subunit, between heptad repeat 1 and 2.  
 239 Mutations R203K-G204R in N gene were always simultaneously detected. It appears that these  
 240 mutations discontinue a serine-arginine (S-R) dipeptide by introducing a lysine in-between them,  
 241 having impacts on structure and function in the mutated N protein.

242 Fifty two sequences in our dataset carried these mutations, particularly 11 of the 59 whole  
 243 genome newly characterized; six of these were from Tuscany, four from Milan and one from Padua.

244

245 Table 3. SARS-CoV2 mutations identified in Italian strains.

Genome region	Mutation	n/total	Percentage (%)
ORF 1ab	S443F	2/135	1.5
	H3076Y	2/135	1.5
	L3606F	3/131	2.3
	P4715L	133/136	97.8
	E5689D	2/135	1.5
	R5919K	2/123	1.6
S	A570D	2/129	1.6
	D614G	128/130	98.5
	G1046V*	3/134	2.2
ORF 3a	G251V	3/134	2.2
M	D3G	21/133	15.8
ORF 7a	G70C	2/134	1.5
N	R203K-G204R	52/133	39.1
	V246I	3/136	2.2

\* mutation under significant selective pressure

246

247

#### 248 3.4 Time reconstruction of the SARS-CoV-2 Italian lineage B.1 phylogeny

249

250

251

Root-to-tip regression analysis of the temporal signal from the Italian B.1 subset revealed a weak association between genetic distances and sampling days (a correlation coefficient of 0.31 and a coefficient of determination ( $R^2$ ) of  $9.9 \times 10^{-2}$ ).

252

253

254

255

256

257

258

Comparison by BF test of the marginal likelihoods obtained by path sampling (PS) and stepping stone sampling (SS) of the strict vs relaxed molecular clock (uncorrelated log-normal) showed that the second performed better than the former (strict vs. relaxed molecular clock BF(PS)=-71.9 and BF(SS)=-71.4 for relaxed clock). Comparison of the different demographic models showed that the BSP and the exponential growth models best fitted the data (BSP vs. constant population size BF(PS)= 27.9 and BF(SS)= 30.2 for BSP; constant population size vs. exponential growth BF(PS)= 7.3 and BF(SS)= 8.6) (Table S3).

259

260

261

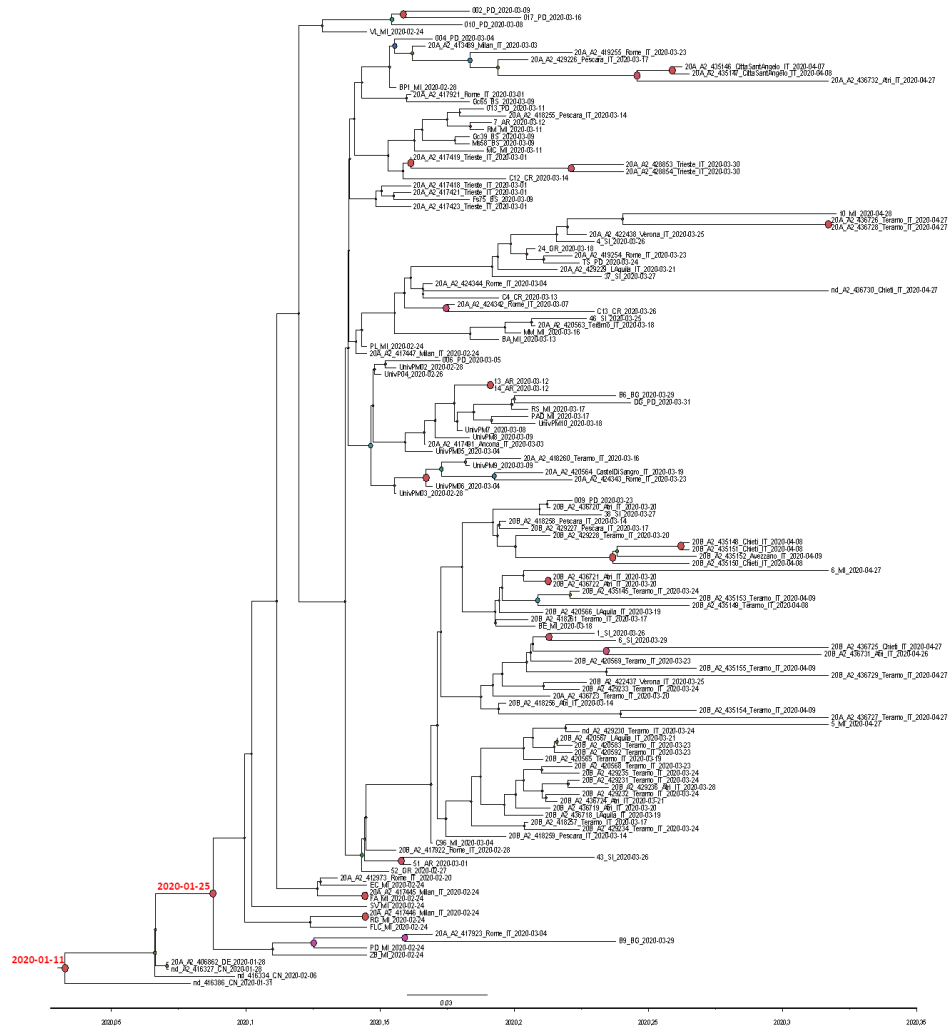
262

The mean tMRCA of the tree root (Figure 2) was estimated at 107 days before present (BP) (95%HPD: 91.2-113.1), corresponding to January 11 2020 (from January 5 to January 27). The tMRCA of the subclade including all the Italian sequences was estimated to be 92.4 (95%HPD: 76.6-95) days BP, corresponding to January 25 (between January 23 and February 10).

263

264

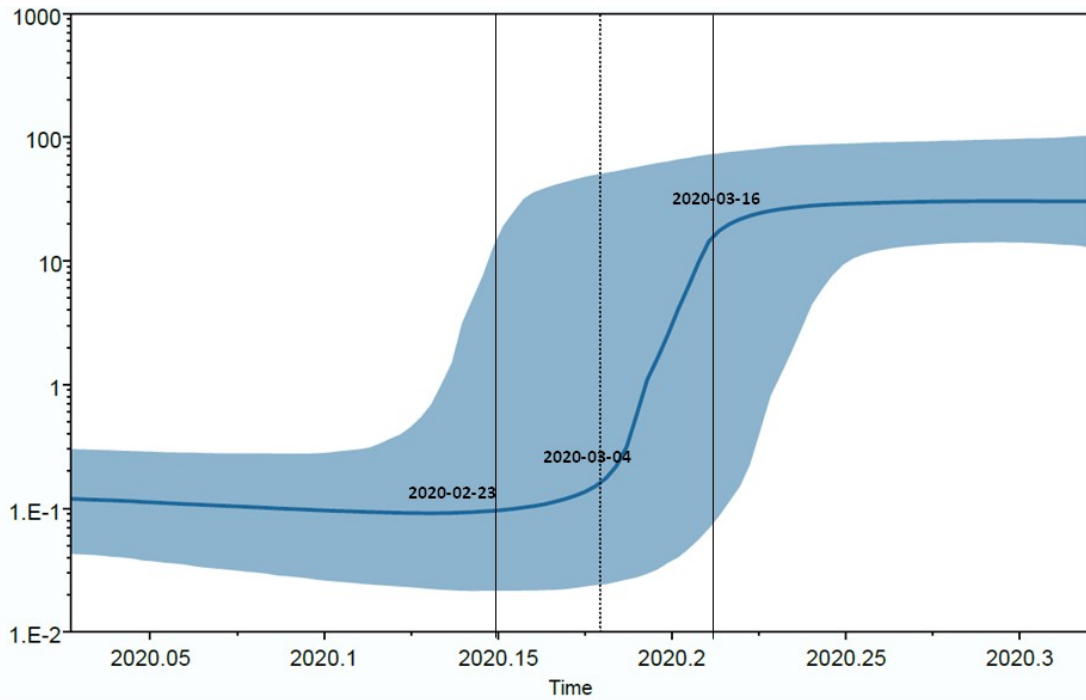
The Bayesian tree of the Italian sequences showed 15 small significant subclades including two to ten isolates (Figure 2).



265  
 266 Figure 2. SARS-CoV-2 tree of 136 Italian strains plus one German and three Chinese isolates from Shanghai,  
 267 showing statistically significant support for clades along the branches (posterior probability > 0.7). Large red  
 268 and purple circles indicated highest posterior probability. Calendar dates of the tree root and the Italian clade  
 269 were showed in red.

270  
 271 *3.5 Phylodynamic analysis of the Italian dataset*

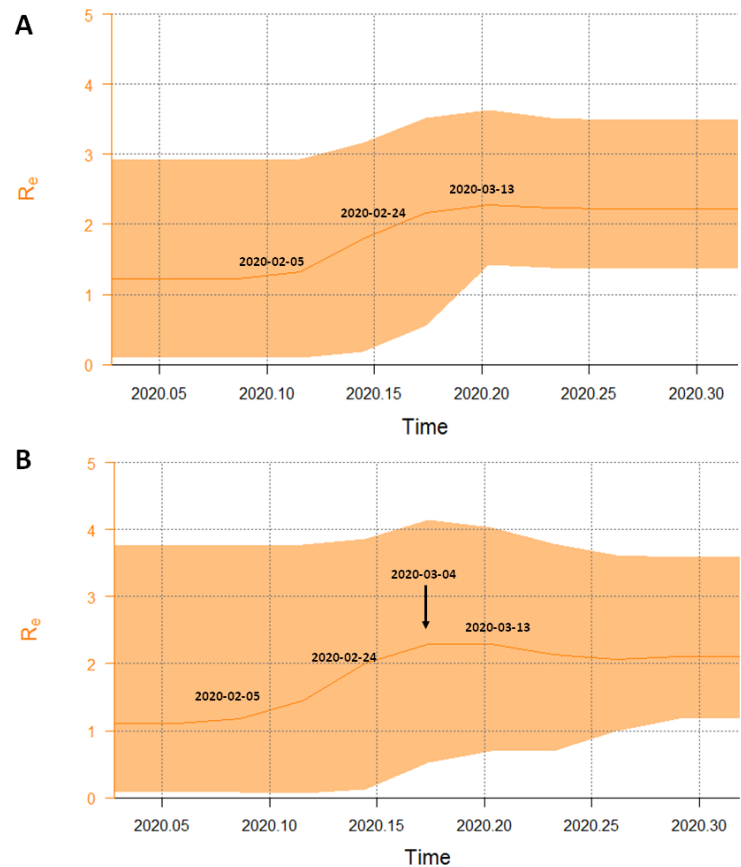
272 The Bayesian skyline plot of the Italian isolates showed an increase in the number of infections  
 273 in the period between 23 February and mid-March 2020, with a rapid exponential growth between  
 274 March 4 and 16 when it reached a plateau continuing until the last sampling time (Figure 3).



275  
 276 Figure 3. Bayesian Skyline plot of the SARS-CoV-2 outbreak. The Y axis indicates effective population size ( $N_e$ )  
 277 and the X axis shows the time in fraction of years. The thick solid line represents the median value of the  
 278 estimates, and the grey area the 95% HPD.

279  
 280 The Bayesian birth-death skyline plot of the  $R_e$  estimates with 95%HPD with a single R group  
 281 (corresponding to  $R_0$ ) estimated a mean value of 2.25 (1.5-3.1). Figure 4 (panels a and b) shows the  
 282 changes of  $R_e$  since the origin of the epidemic and suggests that  $R_e$  was higher than 1 since the early  
 283 days (mean initial  $R_e=1.4$ , 95%HPD: 0.08-2.9). The curve started to grow in early February and  
 284 peaked to a mean value of 2.3 (95%HPD: 1.5-3.5) in the first half of March, and has since remained  
 285 at this value. The curve obtained with three  $R_e$  groups showed a slight decrease at mid-March (Figure  
 286 4, panel b).

287 The origin of the epidemic was estimated at a mean 80.3 days BP (credibility interval: 60-109),  
 288 corresponding to February 7 (between January 9 and February 27). The recovery rate was estimated  
 289 about 7.26 days (CI 4.7-16.0 days), and the transmission rate ( $\lambda$ ) increased from 71.7 to 115.96 in units  
 290 per year (corresponding to a growth rate of 0.06 and 0.18 year<sup>-1</sup>). On the basis of these data, the  
 291 doubling time decreased from 5.1 days to 3.1 days in the period between early February and  
 292 mid-March.



293  
 294 Figure 4. Part A: Birth-death skyline plot of the SARS-CoV-2 outbreak allowing one  $R_e$  intervals. Part B:  
 295 Birth-death skyline plot of the SARS-CoV-2 outbreak allowing three  $R_e$  intervals.  
 296 The curves and the orange areas show the mean  $R_e$  values and their 95% confidence intervals. The Y and X axes  
 297 indicate R values and time in years, respectively.

#### 298 4. Discussion

299 Molecular tracing of SARS-CoV-2 coupled with advanced Bayesian and Maximum likelihood  
 300 phylogenetic analysis provide detailed information about the epidemiology and evolution of  
 301 emerging infections and helps to improve our understanding on the mechanisms of spreading of the  
 302 epidemic.

303 In a previous study [1], we characterized the viral sequences obtained from the first three  
 304 patients coming from the Codogno area who were hospitalized at the very beginning of the  
 305 epidemic in Italy. The Codogno strains correlated with an isolate from an outbreak occurred in  
 306 Bavaria around January 20 [4]. The present analysis shows that all but one of 62 SARS-CoV-2  
 307 sequences obtained from February 22 to the end of April in different Northern and Central Italian  
 308 areas belong to a single clade, corresponding to the Pangolin lineage B.1, the old Nextstrain subclade  
 309 A2a and the new Nextstrain clades 20A and 20B  
 310 (<https://nextstrain.org/blog/2020-06-02-SARSCoV2-clade-naming>) [12], [1]. About 1 out of 4 isolates  
 311 were classified in different clusters, always included in the main B.1 lineage (such as B.1.1 and B.1.5),  
 312 most on a temporal basis, being these clusters more represented among the genomes sampled in the  
 313 second half of March and April (9/14, 64%), while B.1 lineage was more represented in the genomes  
 314 obtained in February and first half of March (33/47, 70.2%).

315 This observation was also confirmed by other Italian studies [3], [1]. The same clade is now the  
 316 most widespread in the world and includes most of the published genomes [5]. The genetic  
 317 distances among the Italian strains were relatively short, corresponding to an average of about 6.4  
 318 mutations per viral genome, even if single isolates may have a higher number of changes. After  
 319 grouping the sequences according with the sampling months, while the within group mean genetic  
 320 distances were higher in February compared to subsequent months, the genetic distance between

321 different months increased with time. This observation confirms a continuous evolution of the viral  
322 genome (with the emergence of new divergent variants) mainly driven by genetic drift. No  
323 significant difference was observed between the non-synonymous and the synonymous  
324 substitutions ( $dn/ds=0.8$ ), suggesting the absence of relevant selective forces driving the evolution of  
325 the viral genome. This observation is further confirmed by the analysis of site-specific selective  
326 pressure in the Italian strains, which only showed a single site under significant positive selection in  
327 the S protein (position 1,046) observed in three strains from Padua. Including in the phylogenetic  
328 tree 3 isolates from Shanghai and one from the first patient of the Bavarian cluster, being at the root  
329 of the B.1 lineage, the dated tree obtained suggests that SARS-CoV-2 entered Italy between late  
330 January and early February 2020. This timing matches with the first autochthonous European cluster  
331 of SARS-CoV-2 transmission in Bavaria (Germany), originated on January 20 [21], [4], [1] by the  
332 introduction of a strain carried by the index patient coming from Shanghai, where the virus had  
333 been circulating since January. The skyline plot analysis of the Italian clade shows an exponential  
334 increase of the effective number of infections from late February to mid-March, in excellent  
335 agreement with the known epidemiological data  
336 (<https://www.epicentro.iss.it/coronavirus/sars-cov-2-dashboard>). In particular, a very rapid growth  
337 of the epidemic was detected between the beginning of March and the middle of the same month,  
338 when the curve reaches a plateau up to the end of sampling (27 April). The mean value of  $R_0$  was  
339 estimated as 2.25 (1.5 to 3.1) in the entire period. A similar result was obtained by Stadler et al. on a  
340 smaller sample of 11 sequences mainly from patients with known travel history to Italy  
341 ([https://virological.org/t/phylogenetic-analyses-based-on-11-genomes-from-the-italian-outbreak/4](https://virological.org/t/phylogenetic-analyses-based-on-11-genomes-from-the-italian-outbreak/426)  
342 26). The estimated basic reproduction number ( $R_0$ ) for SARS-CoV-2 has ranged mainly from 2 to 4,  
343 according to the different methods employed for the evaluation [22]. In Italy, values between 2.4 and  
344 3.6 have been estimated in the early phase of COVID-19 epidemic before the control measures were  
345 taken [23], [24], [25]. Predictive mathematical models are fundamental to understand the dynamics  
346 of the epidemic, plan effective control strategies and verify the efficacy of those applied.

347 Using a birth-death skyline, we analysed the changes of  $R_e$  during the epidemic in Italy over the  
348 entire period. We observed that the  $R_e$  was  $>1$  since the first decade of February, suggesting that the  
349 infection was circulating within the population before the first notified (hospitalized) COVID-19  
350 cases. The  $R_e$  skyline plot reached a value of 2.3 in the first days of March, together with the rapid  
351 increase observed in the number of infections by BSP, and slightly decreased thereafter, in  
352 agreement with the official data on the course of the epidemic. Between February and March the  
353 estimated doubling time of the epidemic decreased from 5.1 to 3.1 days. This value was smaller than  
354 that obtained by us for the epidemic in China [26] and might be interpreted as a consequence of a  
355 delayed application of more stringent containment measures in Italy. In fact, a slight decrease of the  
356  $R_e$  value was observed only after mid-March, when a more rigorous social distancing was enforced  
357 across the entire country. The persistence of a  $R_e$  value higher than one until April, in partial contrast  
358 with the epidemiological data (<https://covstat.it/>), could be due to the fact that our estimate was  
359 influenced by the circulation of the virus in the community, which is larger than the number of the  
360 officially registered clinical cases. It is well known that only a small minority of SARS-CoV-2  
361 infections require hospitalization and that in Italy the number of cases of infection has widely  
362 exceeded the number of official reports. In a recent study, the prevalence of anti-SARS-CoV-2  
363 antibodies in asymptomatic blood donors living in Milan was shown to increase from February to  
364 April, when the prevalence reached its maximum (about 7%) [27]. However, in Italy the numbers of  
365 active cases began to decrease only in the second half of April, when the present study had already  
366 been stopped. Further studies on extended data collection will be required to estimate the effects of  
367 the containment measures.

368 The only one genome characterised in our study not belonging to lineage B.1 was isolated in a  
369 76-year-old man living in the province of Padua (Veneto), who survived to serious COVID-19  
370 manifestations despite old age and the presence of several comorbidities. He denied any contact  
371 with infected subjects and did not travel abroad. This virus belongs to the same lineage (B) of the  
372 first 2 cases imported into Italy from the Hubei region, China, at the end of January 2020, before Italy

373 suspended flights from China. The couple landed at the Milan airport and travelled to other  
374 locations in Northern and Central Italy before the onset of symptoms requiring hospitalization in  
375 Rome, but they had not travelled to Padua. Thus, the origin of such a strain remains unexplained  
376 and further investigations are underway to evaluate whether this strain may have played a role in  
377 causing an epidemic, at least locally. It would also be interesting to investigate whether the currently  
378 predominant strain was for some reasons more epidemic than the initial strain, or if the spread of the  
379 latter was limited by random factors.

380 In conclusion, our data show the importance of molecular and phylogenetic evolutionary  
381 reconstruction in the surveillance of emerging infections. Of note, it appears that the outbreak in  
382 Italy, which involved hundreds of thousands of people, is mainly attributable to a single  
383 introduction of the virus and its uncontrolled circulation for a period of about four weeks. These  
384 results reaffirm the strategic importance of continuous surveillance and timely tracing to define and  
385 rapidly implement effective containment measures for a possible second wave of the pandemic.  
386

387 **Author Contributions:** Conceptualization, A.L, G.Z, C.B., M.G. methodology, A.L, G.Z.; software,  
388 A.L, G.Z., A.B.; formal analysis, A.L, G.Z., S.R., A.B.; investigation, A.L., A.B., N.C., I.V., F.D., S.M.,  
389 F.C.; writing—original draft preparation, A.L, G.Z, M.G.; writing—review and editing, A.L, G.Z,  
390 M.G., A.B., C.B; visualization, all authors; supervision, all authors; project administration, G.Z, C.B.,  
391 M.G.; funding acquisition, G.Z, M.G. All authors have read and agreed to the published version of  
392 the manuscript.

393 **Funding:** This research was funded by Fondo straordinario di Ateneo per lo Studio del Covid-19,  
394 University of Milan.

395 **Acknowledgments:** We acknowledge the authors and the originating and submitting laboratories of  
396 the GISAID sequences. The research was conducted under a cooperative agreement between  
397 Università degli Studi di Milano - Medicina del Lavoro e Clinica delle Malattie Infettive del  
398 Dipartimento di Scienze Biomediche e Cliniche "Luigi Sacco", Intesa Sanpaolo and Intesa Sanpaolo  
399 Innovation Center.

400 **Conflicts of Interest:** The authors declare no conflict of interest.

401 **Contributor Information:** SCIRE collaborative Group

402 F Alessandrini<sup>1</sup>, M Andreoni<sup>2</sup>, G Antonelli<sup>3</sup>, S Babudieri<sup>4</sup>, P Bagnarelli<sup>5</sup>, S Bonora<sup>6</sup>, B Bruzzone<sup>7</sup>, G  
403 Brindicci<sup>8</sup>, P Carrer<sup>9</sup>, F Ceccherini<sup>4</sup>, M Codeluppi<sup>10</sup>, A Coluccello<sup>11</sup>, N Coppola<sup>12</sup>, MG Cusi<sup>13,14</sup>,  
404 C Della Ventura<sup>9</sup>, L Di Sante<sup>5</sup>, S Di Giambenedetto<sup>15</sup>, G Di Perri<sup>6</sup>, V Fiore<sup>4</sup>, S Fiorentini<sup>16</sup>, D  
405 Francisci<sup>17</sup>, C Gandolfo<sup>13</sup>, C Gervasoni<sup>18</sup>, V Ghisetti<sup>6</sup>, R Greco<sup>19</sup>, G Guarona<sup>20</sup>, M Iannetta<sup>2</sup>, L Li  
406 Puma<sup>21</sup>, V. Malagnino<sup>2</sup>, G Mancuso <sup>22</sup>, C Mastroianni<sup>3</sup>, I Menozzi<sup>23</sup>, E Milano<sup>8</sup>, A Miola<sup>21</sup>, M  
407 Morganti<sup>23</sup>, L Monno<sup>8</sup>, G Noberasco<sup>20</sup>, G Nunnari<sup>22</sup>, V Onofri<sup>1</sup>, A Orsi<sup>20</sup>, MG Pierfranceschi<sup>11</sup>, S  
408 Pongolini<sup>23</sup>, D Ripamonti<sup>24</sup>, S Rubino<sup>4</sup>, L Ruggerone<sup>21</sup>, D Russignaga<sup>25</sup>, C Sagnelli<sup>12</sup>, M  
409 Sanguinetti<sup>15</sup>, L Sarmati<sup>2</sup>, L Sasset<sup>26</sup>, E Scaltriti<sup>23</sup>, R Schiavo<sup>10</sup>, M Schioppa<sup>27</sup>, S Testa<sup>11</sup>, C Turchi<sup>1</sup>,  
410 O Turriziani<sup>3</sup>, E Venanzi Rollo<sup>22</sup>, S Zanussi<sup>28</sup>, A Zoncada<sup>11</sup>

411 1. Section of Legal Medicine, Polytechnic University of Marche, Ancona, Italy

412 2. University of Rome Tor Vergata, Rome, Italy

413 3. Laboratory of Virology, Department of Public Health and Molecular Medicine, Sapienza  
414 University, Rome, Italy.

415 4. Department of Medical, Surgical, and Experimental Sciences, University of Sassari, Viale San  
416 Pietro 43, 07100 Sassari, Italy

417 5. Department of Biomedical Sciences and Public Health, Virology and Legal Medicine  
418 Laboratories, Polytechnic University of Marche, Ancona, Italy

- 419 6. Clinic of Infectious Diseases, Amedeo di Savoia Hospital, University of Torino
- 420 7. Hygiene Unit, IRCCS AOU San Martino-IST, Genova, Italy
- 421 8. University Hospital Consortium of the Polyclinic of Bari, Bari, Italy
- 422 9. Department of Biomedical and Clinical Sciences "L. Sacco" University of Milan, IT-20157 Milan,
- 423 Italy
- 424 10. Health Unit of Piacenza, Piacenza, Italy
- 425 11. Unit of Infectious Diseases, Territorial Social Health Company of Cremona, Cremona, Italy
- 426 12. Department of Mental Health and Public Medicine, Section of Infectious Diseases, University of
- 427 Campania Luigi Vanvitelli, Naples, Italy
- 428 13. Department of Medical Biotechnologies, University of Siena, Siena, Italy
- 429 14. Microbiology and Virology Unit, Siena University Hospital, University of Siena, Italy
- 430 15. Institute of Clinical Infectious Diseases, Catholic University of Sacred Heart, Rome, Italy
- 431 16. Laboratory of Microbiology and Virology, Territorial social health company Spedali Civili,
- 432 Department of Molecular and Translational Medicine, University of Brescia, Italy
- 433 17. Infectious Diseases Clinic, Department of Medicine, University of Perugia, Perugia, Italy
- 434 18. ASST Fatebenefratelli Sacco, III Division of Infectious Diseases, University of Milan
- 435 19. Microbiology Unit, Clinical Pathology Complex Operative Unit, Sant'Anna e San Sebastiano
- 436 Hospital, Caserta, Italy
- 437 20. Department of Health Sciences (DISSAL), University of Genoa, Genoa, Italy
- 438 21. Intesa Sanpaolo Innovation Center, Turin, Italy
- 439 22. Complex Operating Unit, Infectious Diseases, Policlinico Gaetano Martino, University of
- 440 Messina, Italy
- 441 23. Risk Analysis and Genomic Epidemiology Unit, Experimental Prophylactic Zoo Institute of
- 442 Lombardy and Emilia Romagna, Parma, Italy
- 443 24. Infectious Diseases Unit, Territorial Social Health Agency of Bergamo, Papa Giovanni XXIII
- 444 Hospital, Bergamo
- 445 25. Prevention and Protection Service, INTESA S.p.A., Turin, Italy
- 446 26. Infectious and Tropical Diseases, University of Padova-Hospital, Padova, Italy
- 447 27. Simple departmental operating unit of Genetics and molecular biology, AORN S. Anna e S.
- 448 Sebastiano, Caserta, Italy
- 449 28. COS of Medical Oncology and Immunocorrelated Tumors, Oncological Reference Center,
- 450 Aviano, Italy

451

## 452 **References**

453

- 454 1. Zehender, G.; Lai, A.; Bergna, A.; Meroni, L.; Riva, A.; Balotta, C.; Tarkowski, M.; Gabrieli, A.; Bernacchia,
- 455 D.; Rusconi, S., et al. Genomic characterization and phylogenetic analysis of SARS-COV-2 in Italy. *Journal*
- 456 *of medical virology* **2020**, *29*, 25794.
- 457 2. Capobianchi, M.R.; Rueca, M.; Messina, F.; Giombini, E.; Carletti, F.; Colavita, F.; Castilletti, C.; Lalle, E.;
- 458 Bordi, L.; Vairo, F., et al. Molecular characterization of SARS-CoV-2 from the first case of COVID-19 in
- 459 Italy. *Clin Microbiol Infect* **2020**, *26*, 954-956.
- 460 3. Stefanelli, P.; Faggioni, G.; Lo Presti, A.; Fiore, S.; Marchi, A.; Benedetti, E.; Fabiani, C.; Anselmo, A.;
- 461 Ciammaruconi, A.; Fortunato, A., et al. Whole genome and phylogenetic analysis of two SARS-CoV-2
- 462 strains isolated in Italy in January and February 2020: additional clues on multiple introductions and
- 463 further circulation in Europe. *Euro Surveill* **2020**, *25*, 1560-7917.

- 464 4. Rothe, C.; Schunk, M.; Sothmann, P.; Bretzel, G.; Froeschl, G.; Wallrauch, C.; Zimmer, T.; Thiel, V.; Janke,  
465 C.; Guggemos, W., et al. Transmission of 2019-nCoV Infection from an Asymptomatic Contact in  
466 Germany. *The New England journal of medicine* **2020**, *382*, 970-971.
- 467 5. Korber, B.; Fischer, W.M.; Gnanakaran, S.; Yoon, H.; Theiler, J.; Abfalterer, W.; Foley, B.; Giorgi, E.E.;  
468 Bhattacharya, T.; Parker, M.D., et al. Spike mutation pipeline reveals the emergence of a more  
469 transmissible form of SARS-CoV-2. *bioRxiv* **2020**, 2020.2004.2029.069054.
- 470 6. Kearse, M.; Moir, R.; Wilson, A.; Stones-Havas, S.; Cheung, M.; Sturrock, S.; Buxton, S.; Cooper, A.;  
471 Markowitz, S.; Duran, C., et al. Geneious Basic: an integrated and extendable desktop software platform  
472 for the organization and analysis of sequence data. *Bioinformatics* **2012**, *28*, 1647-1649.
- 473 7. Katoh, K.; Standley, D.M. MAFFT Multiple Sequence Alignment Software Version 7: Improvements in  
474 Performance and Usability. *Molecular Biology and Evolution* **2013**, *30*, 772-780
- 475 8. Kumar, S.; Stecher, G.; Li, M.; Nknyaz, C.; Tamura, K. MEGA X: Molecular Evolutionary Genetics Analysis  
476 across Computing Platforms. *Mol Biol Evol.* **2018**, *35*, 1547-1549
- 477 9. Martin, D.P.; Murrell, B.; Golden, M.; Khoosal, A.; Muhire, B. RDP4: Detection and analysis of  
478 recombination patterns in virus genomes. *Virus Evolution* **2015**, *1*.
- 479 10. Posada, D. jModelTest: phylogenetic model averaging. *Mol Biol Evol* **2008**, *25*, 1253-1256.
- 480 11. Stamatakis, A. RAXML version 8: a tool for phylogenetic analysis and post-analysis of large phylogenies.  
481 *Bioinformatics* **2014**, *30*, 1312-1313.
- 482 12. Rambaut, A.; Holmes, E.C.; Hill, V.; O'Toole, Á.; McCrone, J.T.; Ruis, C.; du Plessis, L.; Pybus, O.G. A  
483 dynamic nomenclature proposal for SARS-CoV-2 to assist genomic epidemiology. *bioRxiv* **2020**,  
484 2020.2004.2017.046086.
- 485 13. Suchard, M.A.; Lemey, P.; Baele, G.; Ayres, D.L.; Drummond, A.J.; Rambaut, A. Bayesian phylogenetic  
486 and phylodynamic data integration using BEAST 1.10. *Virus Evol* **2018**, *4*, vey016.
- 487 14. Bouckaert, R.; Vaughan, T.G.; Barido-Sottani, J.; Duchêne, S.; Fourment, M.; Gavryushkina, A.; Heled, J.;  
488 Jones, G.; Kühnert, D.; De Maio, N., et al. BEAST 2.5: An advanced software platform for Bayesian  
489 evolutionary analysis. *PLoS computational biology* **2019**, *15*, e1006650.
- 490 15. Rambaut, A.; Lam, T.T.; Max Carvalho, L.; Pybus, O.G. Exploring the temporal structure of  
491 heterochronous sequences using TempEst (formerly Path-O-Gen). *Virus Evol.* **2016**, *2*, 2057-1577.
- 492 16. Baele, G.; Lemey, P.; Bedford, T.; Rambaut, A.; Suchard, M.A.; Alekseyenko, A.V. Improving the accuracy  
493 of demographic and molecular clock model comparison while accommodating phylogenetic uncertainty.  
494 *Mol Biol Evol* **2012**, *29*, 2157-2167.
- 495 17. Suchard, M.A.; Weiss Re Fau - Sinsheimer, J.S.; Sinsheimer, J.S. Bayesian selection of continuous-time  
496 Markov chain evolutionary models. *Mol Biol Evol.* **2001**, *18(6)*, 1001-1013.
- 497 18. Stadler, T.; Kühnert, D.; Bonhoeffer, S.; Drummond, A.J. Birth-death skyline plot reveals temporal changes  
498 of epidemic spread in HIV and hepatitis C virus (HCV). *Proc Natl Acad Sci U S A* **2013**, *110*, 228-233.
- 499 19. Li, Q.; Guan, X.; Wu, P.; Wang, X.; Zhou, L.; Tong, Y.; Ren, R.; Leung, K.S.M.; Lau, E.H.Y.; Wong, J.Y., et al.  
500 Early Transmission Dynamics in Wuhan, China, of Novel Coronavirus-Infected Pneumonia. *New England*  
501 *Journal of Medicine* **2020**, *382*, 1199-1207.
- 502 20. Walker, P.R.; Pybus, O.G.; Rambaut, A.; Holmes, E.C. Comparative population dynamics of HIV-1  
503 subtypes B and C: subtype-specific differences in patterns of epidemic growth. *Infect Genet Evol* **2005**, *5*,  
504 199-208.
- 505 21. Spiteri, G.; Fielding, J.; Diercke, M.; Campese, C.; Enouf, V.; Gaymard, A.; Bella, A.; Sognamiglio, P.; Sierra  
506 Moros, M.J.; Riutort, A.N., et al. First cases of coronavirus disease 2019 (COVID-19) in the WHO European  
507 Region, 24 January to 21 February 2020. *Euro Surveill* **2020**, *25*, 1560-7917.
- 508 22. Liu, Y.; Gayle, A.A.; Wilder-Smith, A.; Rocklöv, J. The reproductive number of COVID-19 is higher  
509 compared to SARS coronavirus. *Journal of travel medicine* **2020**, *27*.
- 510 23. D'Arienzo, M.; Coniglio, A. Assessment of the SARS-CoV-2 basic reproduction number, R0, based on the  
511 early phase of COVID-19 outbreak in Italy. *Biosafety and Health* **2020**.
- 512 24. Gatto, M.; Bertuzzo, E.; Mari, L.; Miccoli, S.; Carraro, L.; Casagrandi, R.; Rinaldo, A. Spread and dynamics  
513 of the COVID-19 epidemic in Italy: Effects of emergency containment measures. *Proceedings of the National*  
514 *Academy of Sciences* **2020**, *117*, 10484-10491.
- 515 25. Yuan, J.; Li, M.; Lv, G.; Lu, Z.K. Monitoring transmissibility and mortality of COVID-19 in Europe. *Int J*  
516 *Infect Dis* **2020**, *95*, 311-315.
- 517 26. Lai, A.; Bergna, A.; Acciarri, C.; Galli, M.; Zehender, G. Early phylogenetic estimate of the effective  
518 reproduction number of SARS-CoV-2. *Journal of medical virology* **2020**, *92*, 675-679.
- 519 27. Valenti, L.; Bergna, A.; Pelusi, S.; Facciotti, F.; Lai, A.; Tarkowski, M.; Berzuini, A.; Caprioli, F.; Santoro, L.;  
520 Baselli, G., et al. SARS-CoV-2 seroprevalence trends in healthy blood donors during the COVID-19 Milan  
521 outbreak. *medRxiv* **2020**, 2020.2005.2011.20098442.



